PHYSICAL REVIEW B **76**, 121303(R) (2007)

Echo peak-shift spectroscopy of non-Markovian exciton dynamics in quantum wells

S. G. Carter,[1] Z. Chen,[1,2,*] and S. T. Cundiff[1]
[1]*JILA, National Institute of Standards and Technology and University of Colorado, Boulder, Colorado 80309-0440, USA*
[2]*Department of Physics, University of Colorado, Boulder, Colorado 80309-0390, USA*
(Received 20 August 2007; published 28 September 2007)

Three-pulse four-wave mixing is used to observe the loss of system memory for excitons confined in quantum wells. By measuring the photon echo peak shift with pulse delay, we obtain the two-time exciton frequency fluctuation correlation function. Spectral diffusion of localized excitons gives rise to exponential decay of the correlation function, while static inhomogeneity gives an offset. Nonmonotonic behavior during the first few picoseconds indicates complex memory effects due to the interaction of excitons with acoustic phonons.

DOI: 10.1103/PhysRevB.76.121303 PACS number(s): 78.67.De, 42.50.Md, 71.35.−y, 78.47.+p

The optical properties of semiconductor quantum wells (QWs) at low temperatures are dominated by excitons. Optical excitation of a semiconductor at the exciton energy generates a coherent superposition of the exciton state and the crystal ground state. Preservation of this coherence is essential for quantum information applications, and the decoherence mechanisms provide information on scattering processes in semiconductors. The complex dynamics that lead to decoherence also occur in atomic, molecular, and biological systems, which are studied using techniques similar to those discussed here.[1–8]

Relatively long optical coherence times (~70 ps) have been observed for localized excitons in GaAs QWs at low temperatures.[9] Well-width fluctuations inhomogeneously broaden the exciton transition and lead to localized states below the center of the exciton absorption line and delocalized states above center.[10] Optical excitation of this distribution of excitons with varying oscillation frequencies causes the excitons to dephase very rapidly. If the exciton frequencies remain constant in time, this inhomogeneous dephasing can be completely reversed by a photon echo experiment. Interactions that change the exciton frequencies lead to irreversible dephasing. Previous photon echo measurements in QWs were sensitive to the rate at which these interactions occur but did not characterize the fluctuations. Here, we use a powerful technique, three-pulse photon echo peak-shift (3PEPS) spectroscopy, which measures the ability of the system to form a photon echo as a function of time. This technique is sensitive to the duration of the interactions that cause dephasing and uniquely illuminates the coupling between excitons and acoustic phonons.

3PEPS spectroscopy is used extensively in molecular systems to study polarization dynamics in which memory effects are important. These memory effects are due to interactions with finite durations and are quantified by the correlation function of frequency fluctuations, $C(t) = \langle \delta\omega(t)\delta\omega(0)\rangle$. The expression $\delta\omega(t)$ is the instantaneous deviation of an oscillator frequency from the mean, and $\langle\cdots\rangle$ represents an ensemble average. The linear and nonlinear optical properties of a medium are determined by $C(t)$.[11] For Gauss-Markov relaxation, the correlation function takes the form $C(t)=D^2e^{-t/T_c}$, where D is the fluctuation bandwidth and T_c is the correlation time.[11] Homogeneous broadening corresponds to $T_c=0$, in which scattering processes immediately destroy correlations. Inhomogeneous broadening corresponds to $T_c=\infty$, such that frequencies in the distribution are constant in time. For the intermediate regime, in which T_c is nonzero and finite, the dynamics are often considered non-Markovian. Previous studies demonstrate that $C(t)$ can be obtained by 3PEPS spectroscopy and use this technique to measure ultrafast molecular dynamics.[2–7]For this technique, the time delay at which the time-integrated four-wave-mixing (FWM) signal is maximum, τ_{peak}, is measured as a function of a second delay T. $\tau_{peak}(T)$ is directly related to $C(t)$.

In semiconductors, both bulk and heterostructures, four-wave mixing is used extensively to study the coherent dynamics of excitons.[12] There are many theoretical predictions of memory effects in bulk semiconductor and QW exciton systems, primarily due to non-Markovian interactions with acoustic and optical phonons.[13–15] Memory effects in bulk GaAs due to LO-phonon interactions are illustrated by the observation of oscillations in the time-integrated FWM signal.[16] In QWs, memory effects in the exciton-acoustic phonon interaction are inferred from FWM experiments,[17,18] but these experiments do not directly characterize the correlation function. We use 3PEPS spectroscopy in GaAs QWs to obtain the exciton correlation function for a series of temperatures and excitation intensities. This correlation function provides a clearer description of the two main processes that lead to decoherence: migration of excitons from one localized site to another; and the interaction of excitons with acoustic phonons. These interactions are also separated from the effects of static inhomogeneity.

The primary sample consists of ten periods of undoped coupled GaAs QWs of width 10 nm and 12 nm, separated by a 2.5 nm $Al_{0.2}Ga_{0.8}As$ tunnel barrier [Fig. 1(a)]. A 30-period distributed Bragg reflector (DBR) is grown beneath these QWs to act as a mirror for incident near-infrared (NIR) light. The experiments are performed in reflection, but the DBR makes this essentially transmission. For simplicity, the FWM geometry [Fig. 1(b)] is illustrated in transmission, and reflectivity is referred to as transmission. The transmission spectrum in Fig. 1(a), taken at a temperature of 4 K, shows

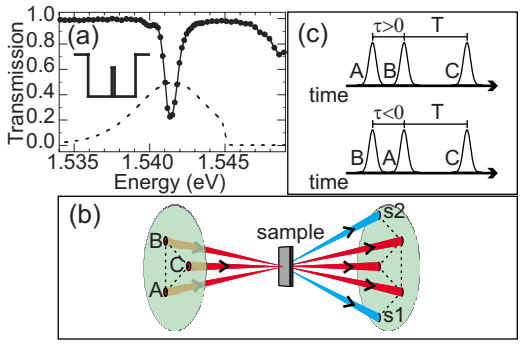

FIG. 1. (Color online) (a) Quantum well transmission spectrum (solid circles and solid line) and typical filtered laser spectrum (dashed line). QW conduction band profile is inset. (b) Three-pulse four-wave-mixing geometry. (c) Pulse timing schematics.

strong absorption at the lowest exciton resonance, which consists of an electron and hole from the lowest conduction and heavy hole valence subbands. A secondary sample consists of ten periods of undoped GaAs QWs of width 10 nm. Due to more extensive measurements in the primary sample, only results from the primary sample are given here.

The NIR pulses are generated by a mode-locked Ti:sapphire laser, with the center wavelength set to 804.3 nm (1.5415 eV) and a spectral bandwidth of 3.0 nm (5.7 meV). The three collinearly polarized pulses (A, B, and C) are focused onto the sample from three corners of an isosceles triangle [Fig. 1(b)]. The average intensity of each beam is typically ~ 2 W/cm^2, corresponding to an exciton density of $\sim 1.7\times 10^9$ cm^{-2} per QW. The first two pulses, A and B, are spectrally filtered to eliminate wavelengths below 802.5 nm (energies above 1.5450 eV). This filtering prevents excitation of higher exciton states or continuum states. A typical filtered laser spectrum is displayed in Fig. 1(a). The filtered (unfiltered) pulse duration is $\sim$370 fs ($\sim$260 fs). The generated FWM signal beams exit the sample in the directions $k_{s1}=-k_A+k_B+k_C$ and $k_{s2}=-k_B+k_A+k_C$.

For a positive delay τ [see the pulse sequence in Fig. 1(c)], pulse A arrives first and generates an exciton polarization, with a distribution of frequencies $\Delta\omega$. The different exciton frequency components dephase on a time scale of $1/\Delta\omega$. Pulse B interacts with each frequency component to form spatially varying population gratings. The optical phase of each component is stored in the spatial phase of each grating for a time T. For $\tau \ll 1/\Delta\omega$ the gratings are spatially in phase so that pulse C immediately diffracts from the gratings into the directions k_{s1} and k_{s2}. For $\tau \gg 1/\Delta\omega$, the gratings are spatially out of phase, but a photon echo can be formed if the phase evolution of the nonlinear polarization induced by pulse C is opposite that of the initial polarization. Thus, a photon echo can occur when pulse C and the first pulse are conjugate, as determined by the relative signs in the output directions. For $\tau>0$, a photon echo can occur in the k_{s1} direction but not in the k_{s2} direction. The opposite is true for $\tau<0$. (See Refs. 1 and 11 for further discussion of photon echo formation.)

Figure 2(a) plots the time-integrated FWM signals in the k_{s1} and k_{s2} directions for $T=0$ ps, with the sample temperature at 2 K. In the k_{s1} direction, for $\tau>0$, a photon echo

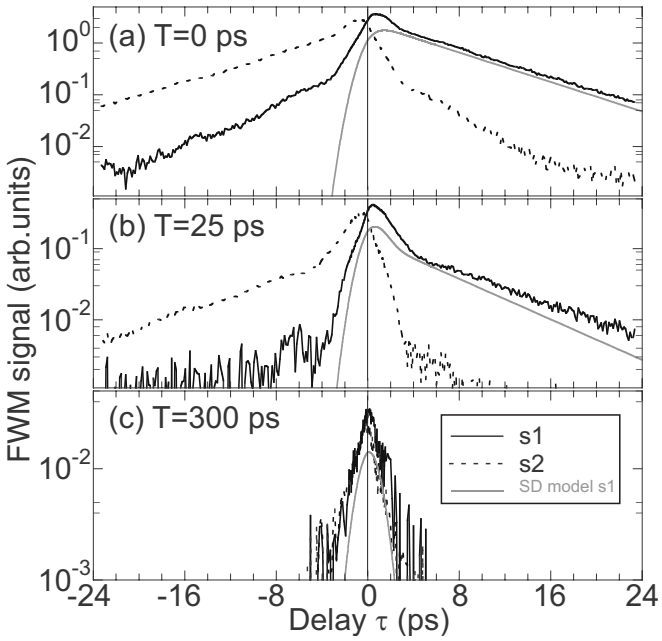

FIG. 2. Time-integrated FWM signals as a function of τ for $T=$ (a) 0, (b) 25, and (c) 300 ps (logarithmic vertical scale). The solid (dashed) lines represent the k_{s1} (k_{s2}) direction. The solid gray lines represent the calculated k_{s1} signal. The vertical lines at the center are at $\tau=0$. The sample temperature is 2 K.

can occur, so the signal decays according to the true decoherence rate γ_{coh}. A fit to $e^{-4\gamma_{coh}\tau}$ after the first 5 ps gives $\gamma_{coh}^{-1}=24.7$ ps.[19] For $\tau<0$, an echo cannot occur, so the signal decays due to inhomogeneity with an initial time constant of ~ 2 ps. The signal in the k_{s2} direction is the same as that in the k_{s1} direction but reflected about $\tau=0$. Asymmetry about $\tau=0$ indicates the formation of a photon echo for one pulse ordering, with the peak position τ_{peak} as a quantitative measure of the ability to form an echo. A finite value of $\tau_{peak}=770$ fs occurs in Fig. 2(a) because a photon echo cannot fully form at $\tau=0$.[19]

The effects of spectral diffusion are observed by varying T. If excitons are able to change frequency during this time, the ability of the system to form an echo is reduced. Figure 2(b) displays the time-integrated FWM signals for $T=25$ ps. During the first 4–5 ps there is rapid decay as spectral diffusion has prevented much of the exciton polarization from forming a photon echo. The remaining portion that can form an echo gives a time constant of $\gamma_{coh}^{-1}=32$ ps. The shift in τ_{peak} to 500 fs represents the loss of system memory. At $T=300$ ps, the signals in Fig. 2(c) are both nearly symmetric about $\tau=0$ with $\tau_{peak}=120$ fs.

The value of τ_{peak} is obtained by fitting the top portion of the $s1$ and $s2$ signals to a parabola.[20] Half the time interval between peaks gives τ_{peak}. The shift in τ_{peak} as a function of T, called the echo peak shift (EPS), is plotted in Fig. 3 for a series of temperatures and excitation intensities. From these 3PEPS measurements, we obtain the exciton correlation function. Previous studies show that for times $T>T_c$, the EPS is proportional to $C(t)$.[2,4,7] Even for $T<T_c$, the EPS and $C(t)$ show the same qualitative behavior. We therefore consider the measured EPS to be proportional to $C(t)$, with some quantitative deviation at short times.

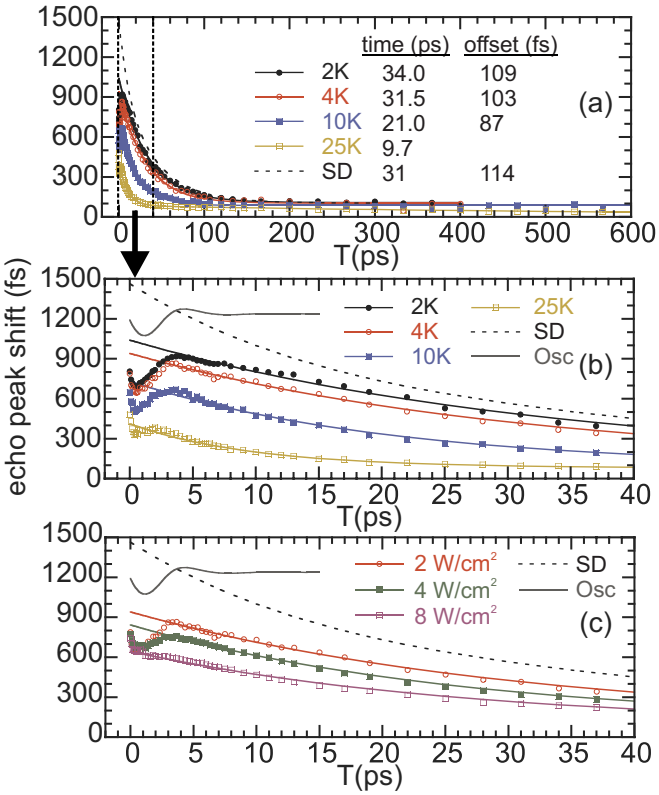

FIG. 3. (Color online) Echo peak shift as a function of T for a series of temperatures (2, 4, 10, and 25 K) at an excitation intensity of 2 W/cm^2 on (a) the full time scale and (b) a 40 ps time scale. (c) EPS as a function of T for a series of excitation intensities (2, 4, and 8 W/cm^2) at a temperature of 4 K on a 40 ps time scale. The markers represent experimental points and the lines represent exponential fits to the data for $T>\sim 5$ ps. The dashed black and solid gray lines represent the calculated EPS from the spectral diffusion (SD) model and the underdamped oscillator (Osc) model, respectively.

The EPS plotted in Figs. 3(a) and 3(b) are measured with sample temperatures from 2 to 25 K at low intensity (2 W/cm^2). At each temperature, there is a sharp decrease in τ_{peak} on the time scale of the pulse width, followed by a slower *increase* on a time scale of a few picoseconds. After ~4 ps, there is an exponential decay to a nearly constant offset of ~100 fs. Exponential fits to the data after 5 ps show that the decay time decreases with temperature from 34 ps at 2 K to 10 ps at 25 K. The offset also decreases a little with temperature until there is no constant offset at 25 K. Instead, at 25 K τ_{peak} decays with a fast (10 ps) and a very slow (~700 ps) time constant. As the excitation intensity is increased from 2 to 8 W/cm^2 at 4 K in Fig. 3(c), the exponential decay and offset remain nearly the same, but the increase in τ_{peak} for small T becomes much less pronounced.

We attribute the exponential decay of the peak shift to the migration of excitons from one localized site to another. Migration of localized QW excitons has been studied a great deal, both experimentally[10,17,21–23] and theoretically.[15,24] At low temperatures, the migration of localized excitons has been shown to be dominated by acoustic-phonon-assisted exciton migration,[21–23] as predicted by theory,[24] with migration times of 10–100 ps. Here, a simple spectral diffusion model is used to describe this exciton migration.[1]

The inhomogeneously broadened exciton system is represented by a distribution of two level systems with varying energy separations $\hbar\omega$. The density of states at a given ω is $g_{sd}(\omega)$, which is estimated as a Gaussian centered at ω_0. The three-pulse FWM signal is obtained by calculating the third-order nonlinear polarization for each exciton frequency. During time T, an exciton at frequency ω' can migrate to another frequency ω with a probability $g_{sd}(\omega)\rho(\omega')/T_{sd}$, where $\rho(\omega)$ is the exciton population at ω, and T_{sd} is the spectral diffusion time. In the limit of δ-function laser pulses, an analytic expression for the FWM signal is obtained by integrating over the distribution, as performed in Ref. 1. Static inhomogeneity is included by integrating this analytic FWM expression over a Gaussian distribution of center frequencies with full width half maximum $\delta\omega_{static}$. By numerically integrating the calculated signal in the k_{s1} direction, the model FWM signals and EPS curves are obtained. The inhomogeneous width participating in spectral diffusion, $\delta\omega_{sd}$, is set to the measured exciton linewidth of ~1 meV. To get reasonable agreement between the model and the data at 2 K and low excitation intensity, the other model parameters are set to $\delta\omega_{static}=0.53$ meV, $T_{sd}=50$ ps, and $\gamma_{coh}=0.031$ ps$^{-1}+1/(2T_{sd})$. The amplitude of the calculated FWM signal is adjusted in each part of Fig. 2 to be just lower than the measured FWM signal.

In Fig. 2(a), at $T=0$, both model and experiment show an asymmetry about $\tau=0$ and the slow decay rate ($4\gamma_{coh}$) for $\tau>0$. However, experiment shows an initially faster decay for $\tau>0$ and a relatively slow decay for $\tau<-4$ ps. At $T=25$ ps, both model and experiment have a fast initial decay at $\tau>0$ due to spectral diffusion and a slower decay rate ($4\gamma_{coh}$) from the remaining excitons able to form an echo. At $T=300$ ps the model and experiment are both nearly symmetric about $\tau=0$ with no slower decay above the experimental noise level.

The calculated EPS shows a roughly exponential decay with a small offset, as seen experimentally. The decay is due to spectral diffusion and the offset is due to static inhomogeneity. The calculated initial value of τ_{peak} is 1.5 ps, much higher than observed experimentally. This discrepancy is partly due to non-Markovian exciton-phonon dynamics (discussed below) and probably also due to fast scattering of delocalized excitons. Fast scattering reduces the system memory on a time scale shorter than the pulsewidth so that it cannot be fully resolved. The initial rapid decay in the EPS is consistent with this explanation. The decrease in the initial value of τ_{peak} with temperature is due to faster decoherence as the thermal occupation of acoustic phonons increases. Similarly, the exponential decay rate for $T>\sim 5$ ps, attributed to exciton migration, increases with temperature, which is consistent with acoustic phonon mediated exciton migration.

Perhaps the most intriguing feature of the measured EPS is the increase in τ_{peak} during the first few picoseconds. To ensure that this feature is not unique to this sample, 3PEPS measurements are performed on the simpler 10 nm GaAs QW sample, which gives the same qualitative behavior but with different time constants. The different QW shapes and degrees of disorder can affect exciton localization and thus

affect interaction with phonons and exciton migration. This increasing EPS cannot be explained by the spectral diffusion model, even if parameters such as T_{sd} and γ_{coh} are made functions of frequency, or if finite pulse effects are included. The spectral diffusion model describes a Gauss-Markov process in which the evolution of the system does not depend on the previous state. This type of process cannot describe the system memory *during* the exciton-phonon interaction.

These non-Markovian dynamics can be addressed by using an underdamped oscillator model,[11] in which acoustic phonons modulate the exciton energy. This single oscillator model is reasonable since excitons in QWs are predicted to interact with acoustic phonons at characteristic frequencies.[24,25] The analytic expression for the FWM signal using this model (δ-function pulse limit) is numerically integrated to obtain τ_{peak} vs T, as displayed in Fig. 3. This model, evaluated at a temperature of 2 K, shows the experimentally observed increasing EPS, with a time scale determined by the frequency of the oscillator. This frequency is set to $\hbar\omega_{ph}=0.7$ meV with a damping rate of $\gamma_{ph}=1$ ps^{-1} to best represent the measured EPS. The exciton-phonon interaction strength was set to reproduce the measured $\gamma_{coh}^{-1}=25$ ps. This oscillator frequency is similar to the value of $\sim$0.4 meV calculated in Ref. 24. Since no exciton migration is included in the underdamped oscillator model, there is no exponential decay of the EPS. Instead, only static inhomogeneity is included in the model, using the measured exciton linewidth of 1 meV. Clearly a model that incorporates both the non-Markovian exciton-phonon interaction and the exciton migration is necessary to fully reproduce the experiment.

3PEPS measurements of QW exciton dynamics provide the correlation function of excitons. A heavily damped oscillation in $C(t)$ during the first 4–5 ps is attributed to the non-Markovian exciton–acoustic-phonon interaction. After the first 4–5 ps, the correlation function decays exponentially with a time constant of 10–30 ps and a small ($\sim$100 fs) offset. This exponential decay is well explained by acoustic-phonon-mediated migration of localized excitons. The offset is due to static inhomogeneity. These results are important for understanding coherent exciton dynamics in semiconductors, in particular for providing a more general description of the scattering processes that lead to decoherence. Measurements of the EPS also provide a unique way to characterize disorder in samples, differentiating between large-scale fluctuations that give a static EPS and microscopic disorder that localizes excitons and gives a decaying EPS.

We thank Andrew S. Huntington and Larry A. Coldren at the University of California, Santa Barbara, for providing our primary sample. We also acknowledge support from the NSF, and S.G.C. acknowledges financial support from the National Research Council.

*Current address: Center for Integrated Nanotechnologies, Los Alamos National Laboratory, Los Alamos, New Mexico 87545, USA.

[1] A. M. Weiner, S. D. Silvestri, and E. P. Ippen, J. Opt. Soc. Am. B **2**, 654 (1985).
[2] M. Cho, J.-Y. Yu, T. Joo, Y. Nagasawa, S. A. Passino, and G. R. Fleming, J. Phys. Chem. **100**, 11944 (1996).
[3] R. Jimenez, F. van Mourik, J. Y. Yu, and G. R. Fleming, J. Phys. Chem. B **101**, 7350 (1997).
[4] W. P. de Boeij, M. S. Pshenichnikov, and D. A. Wiersma, Annu. Rev. Phys. Chem. **49**, 99 (1998).
[5] M. L. Groot, J.-Y. Yu, R. Agarwal, J. R. Morris, and G. R. Fleming, J. Phys. Chem. B **102**, 5923 (1998).
[6] C. J. Fecko, J. D. Eaves, J. J. Loparo, A. Tokmakoff, and P. L. Geissler, Science **301**, 1698 (2003).
[7] A. Piryatinski, C. P. Lawrence, and J. L. Skinner, J. Chem. Phys. **118**, 9672 (2003).
[8] V. O. Lorenz and S. T. Cundiff, Phys. Rev. Lett. **95**, 163601 (2005).
[9] M. D. Webb, S. T. Cundiff, and D. G. Steel, Phys. Rev. Lett. **66**, 934 (1991).
[10] J. Hegarty, L. Goldner, and M. D. Sturge, Phys. Rev. B **30**, 7346 (1984).
[11] S. Mukamel, *Principles of Nonlinear Optical Spectroscopy* (Oxford University Press, New York, 1995).
[12] J. Shah, *Ultrafast Spectroscopy of Semiconductors and Semiconductor Nanostructures* (Springer, New York, 1996).
[13] M. Aihara, Phys. Rev. B **25**, 53 (1982).
[14] D. B. Tran Thoai and H. Haug, Phys. Rev. B **47**, 3574 (1993).
[15] G. Mannarini and R. Zimmermann, Phys. Rev. B **73**, 115325 (2006).
[16] L. Banyai, D. B. Tran Thoai, E. Reitsamer, H. Haug, D. Steinbach, M. U. Wehner, M. Wegener, T. Marschner, and W. Stolz, Phys. Rev. Lett. **75**, 2188 (1995).
[17] H. J. Bakker, K. Leo, J. Shah, and K. Kohler, Phys. Rev. B **49**, 8249 (1994).
[18] Y. Ogawa, A. Iwamatsu, and F. Minami, Phys. Rev. B **73**, 153203 (2006).
[19] T. Yajima and Y. Taira, J. Phys. Soc. Jpn. **47**, 1620 (1979).
[20] The top 85% of the signal is included in the fit for $T<43$ ps; the top 75% is included for 43 ps$\leq T<160$ ps; and the top 65% is included for $T\geq 160$ ps.
[21] H. Wang, M. Jiang, and D. G. Steel, Phys. Rev. Lett. **65**, 1255 (1990).
[22] M. D. Webb, S. T. Cundiff, and D. G. Steel, Phys. Rev. B **43**, 12658 (1991).
[23] S. T. Cundiff and D. G. Steel, IEEE J. Quantum Electron. **28**, 2423 (1992).
[24] T. Takagahara, Phys. Rev. B **31**, 6552 (1985).
[25] J. Hoffmann, M. Umlauff, H. Kalt, W. Langbein, and J. Hvam, Phys. Status Solidi B **204**, 195 (1997).